



RAMAN AND INFRARED RESULTS ON $\text{YBa}_2\text{Cu}_3\text{O}_{7-x}$ TYPE MATERIALS

Gerald Burns,^(a,b) F. H. Dacol,^(a) P. Freitas,^(a)
T. S. Plaskett,^(a) and W. König^(b)

^(a) IBM T. J. Watson Research Center
Yorktown Heights, NY 10598, USA

^(b) Max-Planck-Institut für Festkörperforschung,
Heisenbergstrasse 1, D-7000 Stuttgart 80,
Federal Republic of Germany

(Received 16 June by G. Burns)

We report both Raman and infrared results on the same semiconducting $\text{YBa}_2\text{Cu}_3\text{O}_{7-x}$ material. With the appropriate heat treatment, this material can be reversibly changed from an orthorhombic superconductor ($x \approx 0.0$) to a semiconductor ($x > 0.5$). In the semiconducting material it is easier to measure the phonon features using either technique, and we observe almost the number of modes allowed. By simultaneously considering the modes observed by both techniques, using group theory to sort out the modes in both phases, and using projection operators to determine the symmetry adapted vectors, we arrive at an understanding of some of the modes. We find few differences when comparing our results to other measurements in the superconducting phase. The two general conclusions that we arrive at are: 1) splittings of the modes due to lowering the symmetry from tetragonal to the superconducting orthorhombic phase are not observed; 2) no frequency renormalizations, of the type that have been discussed theoretically, are observed.

Recently intense interest has developed in oxides of copper that are superconductors with high transition temperatures.¹ The phonon spectra are of interest in these new materials because phonons, at least traditionally, are thought to mediate the electron-electron interaction which leads to Cooper pairs and the BCS theory.² Raman and infrared spectroscopy can be used to measure the long wavelength (wave vector, $k \approx 0$) values of the phonon frequencies. These techniques are usually highly accurate, so that temperature and sample dependent effects can be studied easily.

We report Raman and infrared measurements in samples of $\text{YBa}_2\text{Cu}_3\text{O}_{7-x}$. For $x \approx 0$, these materials are orthorhombic and superconductors ($T_c > 90$ K) with an unusual crystal structure.¹ However, with certain heat treatments, $x > 0.5$ can be obtained³, and the material is tetragonal, nonsuperconducting, and nonmetallic; it is a semiconductor. The heat treatment results in a rearrangement of oxygen atoms, O_s , on the (2f) position shown in Fig. 1. The subscript "s" stands for special, and the occupation of this site in the two different structures will be discussed below. Here, we only note that the changes as a function of x (structure, oxygen content, and arrangement) are reversible, so that the effects on most of the phonon frequencies are expected to be small. Indeed, this appears to be the case, according to our data.

From an experimental point of view, one of the

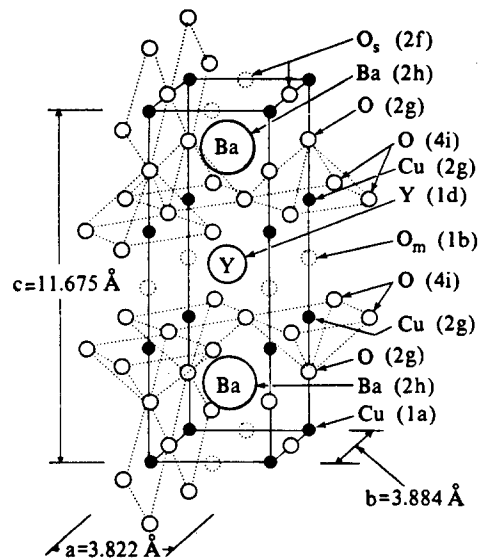


Fig. 1. The crystal structure of $\text{YBa}_2\text{Cu}_3\text{O}_{7-x}$. The orthorhombic unit cell is indicated with different a and b lengths, but the positions of the atoms in the tetragonal structure, with space group $P4/mmm$, are given in Wyckoff notation^{12,13}. See the text for a discussion of the O_s position.

problems with this superconductor is that it is usually produced as a low density ceramic metal. Hence in Raman studies the exciting laser radiation is nonspecularly scattered at the surface, does not penetrate far into the sample, and surface impurities also produce Raman scattering. Although this material is easy to prepare in ceramic form to obtain bulk superconductivity, it is difficult to prepare in high purity form, with stable surfaces for Raman measurements. The work by Rosen, et al.⁴ emphasizes this point. They show that their as prepared $\text{YBa}_2\text{Cu}_3\text{O}_{7-x}$ superconductor ($T_c > 90$ K) gives Raman spectra with many lines due to Y_2BaCuO_5 . This latter material is transparent to the exciting laser light and apparently a strong Raman scatterer.⁴ On the other hand, the $\text{Y}_1\text{Ba}_2\text{Cu}_3\text{O}_{7-x}$ superconductor is a weak Raman scatterer⁵. The weak spectra of the superconductor, coupled with the scattering from impurities, leads to experimental difficulties. Nevertheless, Raman scattering results have been reported by several groups⁵⁻⁸ and although there are differences in the data, many of the features are similar in frequency although not in intensity.

To understand the superconductors, we have taken a different point of view. We started investigated materials having the same K_2NiF_4 structure as the $(\text{La,Ba})_2\text{CuO}_4$ superconductors, but which are insulators. For example,⁹ we have studied Sr_2TiO_4 (and related materials). Our work here on the $\text{YBa}_2\text{Cu}_3\text{O}_{7-x}$ superconductor utilizes the fact that, with the appropriate heat treatment, this material can be made reversibly into a semiconductor. Thus, the Raman and infrared spectra are obtained with greater ease.

Infrared measurements of the superconducting phase are expected to be less affected than Raman scattering because infrared radiation penetrates a metal to a greater depth than the laser light. Indeed, the published^{10,11} infrared results are in reasonable agreement with each other, although there are distinct differences as well. Our infrared measurements on the semiconducting material reveal more lines than the results from the superconductors,^{10,11} almost the number expected from group theory.

The semiconducting samples are prepared by heating orthorhombic superconducting $\text{YBa}_2\text{Cu}_3\text{O}_{7-x}$ ($T_c > 90$ K) to 700 C and slowly cooling it in pure argon. The resistance of the material increases steadily as the temperature is lowered, and is greater than a megohm at room temperature. X-ray structure analysis shows the material is tetragonal with $a = 3.86\text{\AA}$ and $c = 11.79\text{\AA}$. The oxygen content for tetragonal material with similar lattice constants is reported^{3a,12a} by thermoanalytical and chemical reduction techniques to be $x=0.87$ and 0.81 respectively. Neutron measurements indicate that $x \approx 1.0$ ^{12b}.

Structure and symmetry - We give a group theoretical analysis of the normal modes of vibration of the atoms in the tetragonal $\text{YBa}_2\text{Cu}_3\text{O}_{7-x}$ structure. This analysis sorts the normal modes in terms of the irreducible representations of the $4/\text{mmm}-D_{4h}$ point group¹³.

Taking the tetragonal space group as $\text{P}4/\text{mmm}-D_{4h}$, then it is easy to reduce the symmetry to orthorhombic with space group $\text{Pmmm}-D_{2h}$, since this space group is a subgroup of the tetragonal one^{13,14}. Moreover, this procedure has an important advantage over just using the orthorhombic symmetry. Certain normal modes that transform as different irreducible representations in orthorhombic symmetry really are very similar to each other, and transform as the same doubly degenerate (E-type) irreducible representation in the tetragonal symmetry.

The structure^{15,16} of $\text{YBa}_2\text{Cu}_3\text{O}_{7-x}$ is shown in Fig. 1 with various atoms labeled according to the Wyckoff notation^{13,14}. We use the structure derived from the neutron work¹⁶ as it is free from the effects of domains. This figure can be used for the tetragonal phase^{12b} as well as the orthorhombic phase¹⁶ with only small adjustments. We attach an xyz-coordinate system to each atom in this primitive unit cell and apply each space group symmetry operation to find the character of the reducible representation. Reducing this reducible representation yields the irreducible representations listed in Table 1. Since it is a primitive, symorphic^{12,13} space group, this procedure is straightforward.

In both the orthorhombic^{15,16} and tetragonal^{3a,12} structure, the oxygen labeled $\text{O}_m(1b)$ is not observed to be present and is eliminated from further discussions. The oxygens in the plane between the Ba-atoms are more subtle; these are labeled $\text{O}_s(2f)$ in the tetragonal structure, and should be labeled $\text{O}_s(1e)$ in the orthorhombic structure (Table 1). In a defect-free ($x=0$) tetragonal structure, two oxygen atoms occupy these two positions $\text{O}_s(2f)$. However, in the $x > 0.5$ observed^{3a,12} tetragonal structure, at most one half of one oxygen atom is shared by both of these two sites. If $x=1.0$ in the tetragonal phase^{12a}, then no oxygen atoms occupy the $\text{O}_s(2f)$ site. Lastly, in the orthorhombic structure with $x \approx 0.0$, one oxygen atom occupies the one site along the y-axis; this is the $\text{O}_s(1e)$ site. The corresponding site along the a-axis is empty, which gives rise to the orthorhombic, instead of tetragonal, symmetry.

In the tetragonal phase the few defect $\text{O}_s(2f)$ oxygens are probably very weakly bound, resulting in low frequency, disorder broadened, vibrations. Thus, their phonon features probably resemble those found in the fast ion conductors, such as the modes from the disordered Ag-ions in AgI ¹⁷. When counting distinct modes, we ignore these oxygen atoms, which is equivalent to assuming the formula is $\text{YBa}_2\text{Cu}_3\text{O}_{7-x}$ with $x=1$. Sensitive Raman or infrared experiments at lower energies are probably required to observe features from these oxygen atoms. For the fully ordered orthorhombic phase ($x=0.0$) there is no problem; one oxygen atom is located at the (1e) site of the orthorhombic space group, $\text{O}(1e)$ of $\text{O}_s(1e)$, and the result is given in Table 1.

Experimental results - Figure 2 shows the Raman spectrum of the tetragonal, semiconducting material. Although the spectrum is not strong, it is measurable

Table 1 (a) The atoms (At.) in the crystal $\text{YBa}_2\text{Cu}_3\text{O}_{7-x}$ are listed along with their positions, in Wyckoff notation^{12,13} (Wy. Not.), in the tetragonal space group $\text{P4}/\text{mmm}-\text{D}_{4h}^1$, and the orthorhombic space group $\text{Pmmm}-\text{D}_{2h}^1$. For the tetragonal material we assume $x=1$, then the oxygens labeled O_s should be ignored. For the orthorhombic material we assume $x=0.0$, and there is an oxygen at the $1e$ position. For all of the occupied sites for both crystals, the irreducible representations (Irr. Rep.) of the corresponding point groups, which sorts the normal vibrational modes, are given. (b) The sum of the normal modes is given for the two different crystals. These modes are sorted in terms of those that are acoustic modes, infrared active, Raman active, and silent (neither IR or Raman active) modes.

Table 1

(a) $\text{P4}/\text{mmm}-\text{D}_{4h}^1$			$\text{Pmmm}-\text{D}_{2h}^1$	
At.	Wy. Not.	Irr. Rep.	Wy. Not.	Irr. Rep.
Cu	1a	$\text{A}_{2u} + \text{E}_u$	1a	$\text{B}_{1u} + \text{B}_{2u} + \text{B}_{3u}$
Y	1d	ditto	1h	ditto
O	2g	$\text{A}_{1g} + \text{E}_g$ $+ \text{A}_{2u} + \text{E}_u$	2q	$\text{A}_g + \text{B}_{2g} + \text{B}_{3g}$ $+ \text{B}_{1u} + \text{B}_{2u} + \text{B}_{3u}$
Cu	2g	ditto	2q	ditto
Ba	2h	ditto	2t	ditto
O	4i	$\text{A}_{1g} + \text{B}_{1g} + 2\text{E}_g$ $+ \text{A}_{2u} + \text{B}_{2u} + 2\text{E}_u$	2s	ditto
			2r	ditto
O_s	(2f)	$\text{A}_{2u} + \text{B}_{2u} + 2\text{E}_u$	1e	same as 1a

(b) Totals for: $\text{YBa}_2\text{Cu}_3\text{O}_6$		YBa_2CuO_7
Acoustic	$\text{A}_{2u} + \text{E}_u$	$\text{B}_{1u} + \text{B}_{2u} + \text{B}_{3u}$
IR:	$5\text{A}_{2u} + 6\text{E}_u$	$7\text{B}_{1u} + 7\text{B}_{2u} + 7\text{B}_{3u}$
Raman:	$4\text{A}_{1g} + \text{B}_{1g} + 5\text{E}_g$	$5\text{A}_g + 5\text{B}_{2g} + 5\text{B}_{3g}$
Silent:	B_{2u}	---

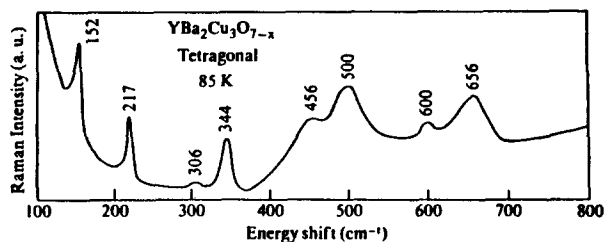


Fig. 2. Raman spectra of tetragonal $\text{YBa}_2\text{Cu}_3\text{O}_{7-x}$.

with a single-channel, double monochromator, using 10 sec. time constants and repeated scans. In the corresponding orthorhombic metal, using the same system, we are not sure that we see any phonon features.

Figure 3 shows the infrared transmission in the same samples of the tetragonal, semiconducting material dispersed in polyethylene. Measurements at room temperature and 10 K show only shifts by a few cm^{-1} . Our corresponding room temperature infrared results in an orthorhombic metallic sample, similarly dispersed, show only a broad absorption throughout this region with a small, sharp absorption at 150 cm^{-1} . (Although, as mentioned, considerable structure is seen in reflectivity from bulk superconductors^{10,11}.) Transmission minima represent absorption maxima which correspond to the phonon frequencies. However, the absorption maxima occur between the transverse and longitudinal optical (TO and LO, respectively) frequencies. For modes with small TO-LO splittings, there is little error, and all but the broad absorption at 360 cm^{-1} fall in this category. Since making these measurements, we have produced larger samples and observed infrared reflectivity. Although we have not, as yet, fit the reflectivity data, there is a precise one to one correspondence between the absorption maxima and the reflectivity bands, indicating the phonon frequencies obtained from the reflectivity will differ little from those given in Fig. 3.

Discussion - Analyzing both Raman and infrared measurements, at the same time, is important in order to reach a better understanding of the results. Furthermore, it is useful to consider the motions of the atoms in the different modes to better appreciate the phonon frequencies and the relationship between the Raman and infrared active modes. To determine the possible motions, we use projection operators which allow the determination of the symmetry adapted vectors¹³.

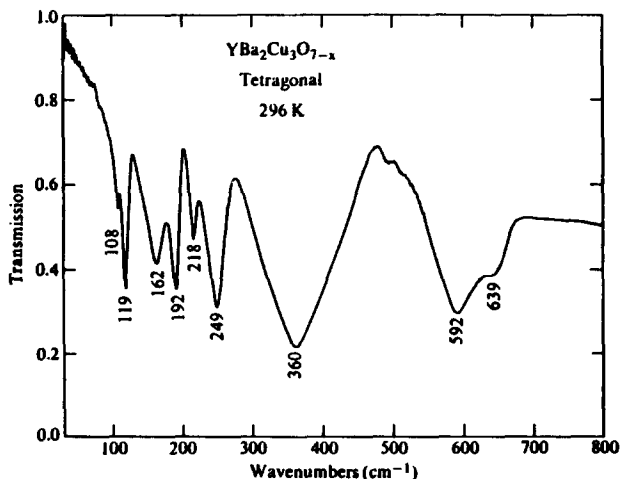


Fig. 3. The infrared transmission of tetragonal $\text{YBa}_2\text{Cu}_3\text{O}_{7-x}$.

Here, we focus on the high frequency vibrations, which should arise from the stretching motion of various Cu-O bonds. First, consider the square planar Cu-O system, which contains the Cu(2g)-O(4i) bonds. In each primitive cell there are two such planes (Fig. 1) which are coupled, and called upper and lower. With the use of projection operators, we determine that the E_g and E_u normal modes of Cu(2g) and O(4i) (Table 1) contain in-plane motion of the Cu against the O; the x-component of probably the highest frequency motion of this Cu(2g)-O(4i) plane is pictured in Fig. 4a. The y-component of these two-fold degenerate modes, not shown, is obvious. Note the similarity of the motions that transform as the E_g and E_u irreducible representations. To the extent that these two Cu-O planes are weakly coupled, the frequency of these Raman and infrared active modes will be close to each other, as also pointed out by Ran, et al.⁸ This observation helps in understanding our Raman and infrared data.

However, there is another high frequency mode involving the stretching of another Cu-O bond. This is the vibration involving Cu(1a) which in the tetragonal material has nearest neighbors of O(2g) and O_s(2f). In the orthorhombic material these bonds are Cu(1a)-O(2q) and Cu(1a)-O_s(1e), remembering that one of the O_s is missing (Table 1). In the orthorhombic material the Cu(1a)-O(2q) bond is already the shortest Cu-O bond length¹⁶. In the tetragonal material, with the population of O_s(2f) severely reduced, this bond be-

comes even shorter^{12a}. Motion that involves compressing the Cu(1a)-O(2g) bond is shown in Fig. 4b. Both a Raman active A_{1g} phonon and an infrared active A_{2u} phonon have this type of Cu-O motion, with movement of the Cu allowed only in the infrared active mode. As in the case discussed involving the Cu(2g)-O(4i) plane, the Raman and infrared modes should have similar frequencies. With these two examples in mind, let us consider the data.

Comparing the high frequency Raman and infrared data of the tetragonal material, we immediately note that both show two features that are correspondingly close in frequency. We associate the highest frequency Raman mode, at 656 cm^{-1} , with the A_{1g} , and the highest frequency infrared mode ($\approx 639\text{ cm}^{-1}$) with the A_{2u} , involving Cu(1a)-O(2g) motion as discussed above (Fig. 4b). Correspondingly, we associate the next highest frequency Raman mode (600 cm^{-1}) with the E_g mode involving in-plane Cu(2g)-O(4i) motion, as discussed above. Its E_u infrared partner ($\approx 592\text{ cm}^{-1}$ Fig. 3) is the next highest infrared mode. The frequencies associated with these assignments are rather close, and they could be reversed. Of course, single crystal polarized Raman and infrared measurements could distinguish between the modes because of the different symmetries. However, the single crystal results published so far⁶ report many fewer modes than expected (Table 1), so the situation is, as yet, not clear.

We can compare our observations in the tetragonal material with those in the metallic orthorhombic phase measured using either Raman⁵⁻⁸ or infrared^{10,11} techniques. Our Raman results of these two highest frequency features are in reasonable agreement with the published ones, although the intensities of the modes in the various papers seem to vary strongly. This may be due to sample preparation. Furthermore, our infrared results of the corresponding two highest-frequency modes agree with other measurements.^{10,11} However, in general we observe more modes than most others, almost as many as predicted by group theory.

In this short paper we have only discussed the highest frequency features; there are many other lower frequency modes. Bending modes of the Cu(2g)-O(4i) plane of the Raman A_{1g} and infrared A_{2u} type occurs. Similarly, bending of the Cu(1a)-O(2g) bond of the Raman E_g and infrared E_u type, will have lower frequencies. In fact, since many modes transform as the same irreducible representations, a mixture of many motions enter into these modes. A complete normal mode calculation is required to sort out the various motions. Nevertheless, we believe our discussion of the highest frequency modes to be fundamentally correct.

Conclusions - From the tetragonal semiconducting $\text{YBa}_2\text{Cu}_3\text{O}_{7-x}$ material, we see almost the number of modes predicted by group theory (Table 1).

We have argued that one of the highest frequency Raman modes in the tetragonal phase, in the $590\text{--}660\text{ cm}^{-1}$ region, is an E_g mode, and the corresponding infrared active mode is an E_u mode. In the metallic,

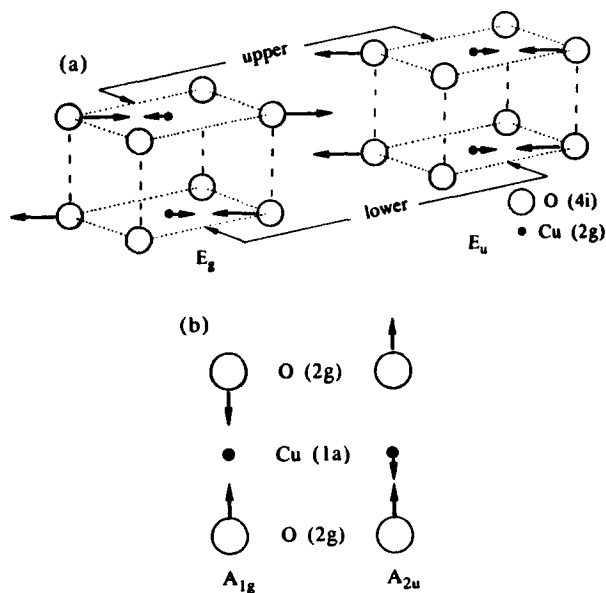


Fig. 4. Symmetry adapted vectors, and probable normal modes, for the high frequency vibrations that involve motion of the Cu against O atoms. (a) shows the motions involving the two planes with Cu(2g)-O(4i) bonds. The motions transform as the E_g and E_u irreducible representations. (b) shows the motions that involves the Cu(1a)-O(2g) bond. The motions transform as the A_{1g} and A_{2u} irreducible representations.

orthorhombic phase, both of these modes should split. Yet neither the published Raman⁵⁻⁸ nor infrared^{10,11} data show a splitting of modes in this region. This implies that the splittings due to the orthorhombic symmetry are small. In looking for such splittings in the lower frequency modes, again, we find no evidence for such splittings. These observations are important when counting the number of distinct one-phonon features. For example, we expect even for the metallic orthorhombic material, 10 Raman and 11 infrared frequencies (as in the tetragonal material), rather than the 15 and 21, respectively, as indicated in Table 1.

This leads to another conclusion. We assume that we are correct in associating the highest frequency features with Cu-O stretching motion in the chains involving Cu(1a)-O(2g) and in the planar Cu(2g)-O(4i) groups. In the metallic orthorhombic superconducting material we might expect, therefore, some large temperature effects¹⁸ associated with electron-phonon coupling and superconductivity². Some small anomalies^{5,19}, of the order of 5 cm^{-1} , have been reported^{5,19}. It remains

to be seen if they are associated with the expected anomalies. Of course, the Raman and infrared active modes are zone center modes. Zone boundary phonons¹⁸, for example due to uniform breathing modes, might play the important role. However, both types of modes involve Cu-O stretching and, therefore, are probably on the same dispersion curves. Thus, if the frequencies of zone boundary modes are renormalized, large effects on the same branch at the zone center would be expected. These observations, in conjunction with the null effect in the isotope shift experiments,^{7,20} further suggests that these high temperature superconductors indeed are novel materials.

Acknowledgements - One of us (G.B.) acknowledges with pleasure an Alexander von Humboldt fellowship, which allowed some of this work to be accomplished. Also the hospitality and stimulation of the Max Planck Institute for Solid State Physics is very gratefully acknowledged.

References

- 1 For a review of the early work in this field, see A. Khurana, *Physics Today* **40**, 17 (1987).
- 2 J. Barden, L. N. Cooper, and J. R. Schriber, *Phys. Rev. B* **108**, 1175 (1957). See any solid state book for a discussion of the BCS theory.
- 3 (a) P. K. Gallagher, H. M. O'Bryan, S. A. Sunshine, D. W. Murphy, *Mat. Res. Bull.*, **22**, 995 (1987). (b) I. Chen, S. Keating, C. Y. Keating, X. Wu, J. Wu, P. E. Reyes-Morel, and T. Y. Tien, *Solid State Commun.*, **63**, 997 (1987). (c) R. Beyers, G. Lim, E. M. Engler, V. Y. Lee, M. L. Ramirez, R. J. Savoy, R. D. Jacowitz, T. M. Shaw, S. La Placa, R. Boehme, C. C. Tsuei, S. I. Park, M. W. Shafer, W. J. Gallagher and G. V. Chandrashekar, *Appl. Phys. Lett.*, to be published.
- 4 H. Rosen, E. M. Engler, T. C. Strand, V. Y. Lee, and D. Bethune, *Phys. Rev. B*, to be published.
- 5 R. M. Macfarlane, H. Rosen, and H. Seki, *Solid State Commun.*, **63**, 831 (1987).
- 6 R. J. Hemley and H. K. Mao, *Phys. Rev. Lett.* **58**, 2340 (1987).
- 7 B. Batlogg, R. J. Cava, A. Jayaraman, R. B. van Dover, G. A. Kourouklis, S. Sunshine, D. W. Murphy, L. W. Rupp, H. S. Chen, A. White, K. T. Short, A. M. Muzsca, and E. A. Rietman, *Phys. Rev. Lett.* **58**, 2333 (1987).
- 8 L. Ran, R. Merlin, M. Cardona, H. Mattausch, W. Bauhofer, A. Simon, F. Garcia-Alvarado, E. Moran, M. Vallet, J. M. Gonzalez-Calbet, and M. A. Alario, *Solid State Commun.*, **63**, 839 (1987).
- 9 G. Burns, F. H. Dacol, and M. W. Shafer, *Solid State Commun.*, **62**, 687 (1987).
- 10 D. A. Bonn, J. E. Greedan, C. V. Stager, T. Timusk, M. G. Doss, S. L. Herr, K. Kamaras, and D. B. Tanner, *Phys. Rev. Lett.* **58**, 2249 (1987).
- 11 L. Genzel, A. Wittlin, J. Kuhl, H. Mattausch, W. Bauhofer, and A. Simon, *Solid State Commun.*, **63**, 843 (1987).
- 12 (a) J. M. Tarascon, W. R. McKinnon, L. H. Greene, G. W. Hall and E. M. Vogel, *Phys. Rev. B*, to be published. (b) A. W. Hewat, J. J. Cappon, C. Chailout, M. Marezio, E. A. Hewat, submitted to *Nature*. (c) If one chooses $a > b$ then O_s should be labeled $\text{O}_s(1b)$.
- 13 a) G. Burns and A. M. Glazer, "Space Groups for Solid State Scientists" (Academic Press, 1978). b) G. Burns "Introduction to Group Theory with Applications" (Academic Press, 1977).
- 14 International Tables for x-ray Crystallography, Vol. I, Ed. N.F.M. Hendry and K. Lonsdale (Kynoch, 1952, 1965, 1968).
- 15 (a) M. T. Siegrist, S. Sunshine, D. W. Murphy, R. J. Cava, and S. M. Zahurak, *Phys. Rev. B* **35**, 7137 (1987). (b) R. M. Hazen, L. W. Finger, R. J. Angel, C. T. Prewitt, N. L. Ross, H. K. Mao, C. G. Hadjidakos, P. H. Hor, R. L. Mang, and C. W. Chu, *Phys. Rev. B* **35**, 7238 (1987).
- 16 (a) J. J. Capponi, C. Chailout, A. W. Hewat, P. Lejay, M. Marezio, N. Nguyen, B. Raveau, J. L. Soubeyrou, J. L. Tholence, and R. Tournier, *Europhys. Lett.* **3**, 1301 (1987). (b) M. A. Beno, L. Soderholm, D. W. Capone, D. G. Hinks, J. D. Jorgensen, Schuller, C. U. Segre, K. Zhang, and J. D. Grace, *Appl. Phys. Lett.*, to be published.
- 17 For example, see R. Alben and G. Burns, *Phys. Rev. B* **16**, 3746 (1977).
- 18 W. Weber, *Phys. Rev. Lett.* **58**, 1371 (1987).
- 19 A. Wittlin, R. Liu, M. Cardona, L. Genzel, W. König, and F. Garcia-Alvarado, *Solid State Commun.*, to be published.

20 L. C. Bourne, M. F. Crommie, A. Zettl, H. C. Loye,
S. W. Keller, K. L. Leary, A. M. Stacy, K. J. Chang,

M. L. Cohen, and D. E. Morris, *Phys. Rev. Lett.* **58**,
2337 (1987).